Cell Tissue Res (2014) 358:359–369
DOI 10.1007/s00441-014-1961-2

REGULAR ARTICLE

Involvement of RhoA/ROCK in insulin secretion of pancreatic β-cells in 3D culture

Xiaofang Liu · Fang Yan · Hailei Yao · Mingyang Chang · Jinhua Qin · Yali Li · Yunfang Wang · Xuetao Pei

Received: 7 May 2014 / Accepted: 3 July 2014 / Published online: 17 August 2014

Abstract Cell-cell contacts and interactions between pancreatic β-cells and/or other cell populations within islets are essential for cell survival, insulin secretion, and functional synchronization. Three-dimensional (3D) culture systems supply the ideal microenvironment for islet-like cluster formation and functional maintenance. However, the underlying mechanisms remain unclear. In this study, mouse insulinoma 6 (MIN6) cells were cultured in a rotating 3D culture system to form islet-like aggregates. Glucose-stimulated insulin secretion (GSIS) and the RhoA/ROCK pathway were investigated. In the 3D-cultured MIN6 cells, more endocrine-specific genes were up-regulated, and GSIS was increased to a greater extent than in cells grown in monolayers. RhoA/ROCK inactivation led to F-actin remodeling in the MIN6 cell aggregates and greater insulin exocytosis. The gap junction protein, connexin 36 (Cx36), was up-regulated in MIN6 cell aggregates and RhoA/ROCK-inactivated monolayer cells. GSIS dramatically decreased when Cx36 was knocked down by short interfering RNA and could not be reversed by RhoA/ROCK inactivation. Thus, the RhoA/ROCK signaling pathway is involved in insulin release through the up-regulation of Cx36 expression in 3D-cultured MIN6 cells.

Keywords Three-dimensional (3D) culture · Insulin release · RhoA · ROCK · Connexin 36 · Mouse pancreatic cell line (MIN6)

Xiaofang Liu, Fang Yan, and Hailei Yao contributed equally to this work

This work was supported by the National High Technology Research and Development Program of China (nos. 2013AA020109 to P.X., 2012AA020501 to W.Y.) the National Nature Science Foundation of China (nos. 81170388 and 31370990 to W.Y.).

Electronic supplementary material The online version of this article (doi:10.1007/s00441-014-1961-2) contains supplementary material, which is available to authorized users.

X. Liu · F. Yan · H. Yao · M. Chang · J. Qin · Y. Wang · X. Pei
Stem Cell and Regenerative Medicine Laboratory, Beijing Institute of Transfusion Medicine, Beijing 100850, China

F. Yan · H. Yao · M. Chang · J. Qin · Y. Wang (✉) · X. Pei (✉)
South China Research Center for Stem Cell & Regenerative Medicine, AMMS, Guangzhou 510005, China
e-mail: wangyf1972@gmail.com
e-mail: peixt@nic.bmi.ac.cn

X. Liu
Department of Obstetrics and Gynecology, General Hospital of Air Force, Beijing 10014, China

Y. Li (✉)
Department of Obstetrics and Gynecology, General Hospital of PLA, Beijing 100039, China
e-mail: li_yali@hotmail.com

Introduction

Pancreatic islets are essential for the maintenance of glucose homeostasis during fasting and feeding. Major components are β-cells that initially appear as scattered cells during embryonic development and then, as development progresses, that aggregate with neighboring β-cells and/or other types of endocrine cells to form pancreatic islets (Bell and Polonsky 2001; Grapin-Botton and Melton 2000). Healthy β-cells continually produce insulin, storing it within granules and steadily releasing small amounts into the blood stream over the course of a day (called basal insulin release). Glucose metabolism autonomously triggers insulin secretion, known as glucose-stimulated insulin secretion (GSIS). Communication between β cells suppresses basal insulin secretion but enhances GSIS ensuring the glucose homeostasis function of pancreatic islets (Luther et al. 2006; Ravier et al. 2005). Progress has been made in exploring the molecular mechanism(s) underlying these processes. Research shows that a number of factors such as glucose metabolism, membrane depolarization, and insulin exocytosis control the GSIS pathway (Ahren and Filipsson 2000; Henquin 2000).

However, the connection between those factors in regulating insulin secretion still requires clarification.

Three-dimensional (3D) cultures can mimic the in vivo microenvironment, enhancing cell-cell and cell-matrix interactions and subsequent cell signaling transmission. A variety of 3D cell culture systems have been developed for directing stem cell differentiation into various lineages (Pelto et al. 2013; Villa-Diaz et al. 2013). Recent research shows that the 3D culture model not only generates more insulin-secreting cells than those in traditional two-dimensional (2D) monolayer conditions, but also makes differentiated cells form islet-like tissue structures that display greater similarities to adult pancreatic islets (Bhandari et al. 2011; Guo-Parke et al. 2012; Wang and Ye 2009).

Insulin secretion is a process of exocytosis by pancreatic β-cells and is regulated by actin cytoskeleton dynamics (Nevins and Thurmond 2003; Thurmond et al. 2003). The three best-characterized members of the small Rho GTPase family, namely Rho, Rac, and Cdc42, all play central roles in the regulation of actin cytoskeleton dynamics and in defined stem cell differentiation (Ridley 2006). Both Cdc42 and Rac are involved in actin cytoskeleton regulation and play a positive role in the stimulated insulin exocytosis of β-cells (Li et al. 2004; Nevins and Thurmond 2003, 2005). Rho is a mediator of insulin signaling and is thereby involved in the development of insulin resistance, the regulation of insulin action, and glucose homeostasis (Furukawa et al. 2005; Song et al. 2009). Rho is activated under diabetic conditions, and the inhibition of Rho activity markedly increases insulin gene transcription (Nakamura et al. 2006). Hammar et al. (2009) have demonstrated that the inhibition of Rho and Rho-associated kinase in primary β-cells culminates in a significant increase in cell spreading, actin depolymerization, and GSIS. However, the potential roles of Rho G protein in insulin secretion remain to be further confirmed, and an evaluation of the regulatory roles for this Rho-sensitive signaling pathway in islet function is possibly needed (Kowluru 2010).

Connexins (Cxs) form cell-to-cell channels that cluster at gap junction domains of the membrane of most cell types and mediate the exchange of small molecules (< 1000 Da) between adjacent cells (Bosco et al. 2011; Scemes et al. 2009). Studies have shown that the presence of gap junctions between β-cells is required for proper control of insulin secretion (Speier et al. 2007). Thus, single β-cells exhibit poor insulin gene expression and produce low amounts of secreted insulin; they barely show an increase in these functions after stimulation. However, restoration of β-cell contacts leads to a rapid improvement in both insulin biosynthesis and release (Meda 1996; Meda et al. 1990). Insulin secretion is a synchronized process of pancreatic β-cells in islets, and these cells set up a signaling system via a gap junction protein, namely connexin 36 (Cx36), to coordinate islet cell functions (Benninger et al. 2011; Michon et al. 2005). Studies have also identified that Cx36 is involved in β-cell differentiation, and loss of Cx36 causes pancreatic dysfunction reminiscent of that observed in human type 1 and type 2 diabetics (Carvalho et al. 2012; Head et al. 2012; Ravier et al. 2005).

In the present study, we have used mouse insulinoma 6 (MIN6) cell lines to verify the efficacy of the 3D culture system in GSIS and to explore the roles of RhoA/ROCK and Cx36 in exocytosis and in the synchronization of cells in the 3D culture system. We have attempted to discover the RhoA and Cx36 relationship that might suggest a mechanism that initiates insulin secretion in MIN6 cell clusters and the maintenance of functions in a 3D culture system.

Materials and methods

Cell culture The mouse pancreatic cell line, MIN6, was cultured in Dulbecco's modified Eagle's medium (DMEM; Invitrogen, Paisley, UK). The DMEM contained 25 mmol/l glucose, supplemented with 15 % fetal bovine serum (Invitrogen), 100 U/ml penicillin (Invitrogen), 100 μg/ml streptomycin, and 50 μM β-mercaptoethanol (Invitrogen) in a humidified atmosphere at 37 °C with 5 % CO_2. The medium was changed every 2 days. MIN6 cells at no more than passage 25 were used because, after that passage, the MIN6 cells had lost certain functions and had decreased insulin content. For 3D cultures, the MIN6 cells were seeded into ultra-low-attachment 24-well plates at a density of 1.5×10^5 cells/well and incubated at 37 °C with 5 % CO_2 on 3D rotators (Edmund Bühler GmbH, Germany) set at 80–100 rpm. For 2D cultures, cells were seeded into tissue culture plates (24-well plates) at a density of 1.5×10^5 cells/well.

Chemical inhibition of Rho and ROCK To inhibit the activity of Rho, cells were treated with cell-permeable C3 transferase (C3T; 2 μg/ml; Cytoskeleton, USA). The activity of ROCK was inhibited by the small molecule Y-27632 (Stemgent, USA). For long-term assays, cells were treated with inhibitors for 4 days, whereas for short-term assays, the inhibitors were added for only 2 h during the insulin secretion test. Y27632 was diluted in dimethylsulfoxide (DMSO; Invitrogen, USA) as a stock solution, and the same volume of DMSO was added to the control group.

Lentiviral packaging and transduction The RhoA-positive (constitutively active, CA) and negative mutant (dominant negative, DN) mutant plasmids were constructed as previously published (Yao et al. 2009). Briefly, mutant plasmids were subcloned into the lentiviral vector pBPLV. An empty pBPLV vector was used as a control. Lentiviruses were established in 293FT cells by using packaging plasmids (pLP1, pLP2, and pLP/VSVG; Invitrogen) and Lipofectamine 2000. Viruses were harvested after 48–72 h and were used for the infection of MIN6 cells overnight in the presence of 5 μg/ml polybrene. Cells positive for green fluorescent protein were sorted by fluorescence-activated cell sorting and used for the experiments described below.

Insulin secretion assay The MIN6 cells, including gene-modified and chemically treated cells, were cultured for 4 days under either 2D or 3D conditions. Before the insulin secretion test, cells were pre-incubated in DMEM containing 5 mM glucose for 16–24 h. The cells were incubated in basal medium, namely Krebs-Ringer bicarbonate HEPES (KRBH) supplemented with 2 mM glucose, at 37 °C for 1 h and changed into fresh basal medium for another 1 h of incubation. The cells were then transferred into a stimulating condition (KRBH supplemented with 20 mM glucose) for 1 h of incubation at 37 °C. The supernatant was collected for enzyme-linked immunosorbent assay (ELISA) or stored at −80 °C. The RhoA and ROCK inhibitors were added as noted in the Results. Cells were collected, after which the proteins were extracted with RIPA, and total protein content was determined by Bradford assays. The amount of insulin in the supernatant and/or cell extracts was measured by a mouse insulin ELISA kit (Mercodia, Winston Salem, N.C., USA). Insulin secretion was normalized against the protein content of the cell lysate.

RNA extraction and real-time quantitative polymerase chain reaction Total RNAs were extracted by using an RNeasy mini kit (QIAGEN, Valencia, Calif., USA) according to the manufacturer's protocols. We synthesized cDNA from 2 μg RNA with M-MLV reverse transcriptase and oligo-DT according to the manufacturer's instructions (TaKaRa Bio, Otsu, Japan). Real-time polymerase chain reaction (PCR) was performed by using a real-time quantitative PCR (Q-PCR) detection system (Bio-Rad IQ5 System, Bio-Rad Laboratories, USA). Briefly, the Q-PCR system consisted of a 3-min denaturing step at 95 °C followed by 40 cycles at 95 °C for 15 s and 58 °C for 30 s. A melt analysis was performed following each Q-PCR run. We used D-glyceraldehyde-3-phosphate dehydrogenase expression as an internal control. The Q-PCR primer sequences used are listed in Supplementary Table 1.

Western blotting assay and pull-down assay The inhibitor-treated or control MIN6 cells were lysed overnight with cold RIPA buffer containing combinations of proteinase inhibitors. The lysates were then centrifuged at 12,000 rpm for 20 min to remove insoluble materials, and the concentration of protein was determined by Bradford assays. Proteins were separated in 12 % SDS–polyacrylamide gradient gels and transferred onto polyvinylidene difluoride membranes (Millipore, Bedford, Mass., USA). The membranes were blocked with 5 % nonfat milk in TRIS-buffered saline at room temperature for 1 h and incubated with anti-Cx36 antibody (1:500; Abcam, Cambridge, UK) and anti-β actin antibody (1:1000; Santa Cruz, USA) overnight at 4 °C. The membranes were incubated with a secondary antibody conjugated with horseradish peroxidase for 1 h at room temperature, and the target protein bands were detected by an enhanced chemiluminescence labeling kit (Santa Cruz) according to the manufacturer's instructions.

Short interfering RNA syntheses and transfection For Cx36 knockdown, we used transfection with short interfering RNA (siRNA) with lipofectamine-2000 (Invitrogen, USA) on six-well plates according to the manufacturer's protocols, with knockdown efficiencies being determined by Western blotting assay. Three different siRNAs were designed for targeting mouse Cx36, and one siRNA was designed as the negative control. The siRNA sequences are listed in Supplementary Table 2.

Immunofluorescence and F-actin cytoskeleton visualization Monolayers of MIN6 cells were fixed in 4 % paraformaldehyde for 20 min, and multicell spheroids were fixed for 30 min. The cells were then permeabilized with 0.2 % Triton X-100 for 10 min, blocked in phosphate-buffered saline (PBS) containing 1 % bovine serum albumin (BSA) for 1 h, and incubated in primary antibodies overnight at 4 °C. Cells were washed and incubated with secondary antibody for 1 h. After 4 days of culture and treatment with low or high glucose, inhibitor-treated cells were pre-incubated in KRBH buffer for 1 h with 2 mM glucose and then fixed with 4 % paraformaldehyde for 20 min at room temperature immediately or after an additional 5-min treatment with 20 mM glucose and permeabilized with 0.2 % Triton X-100 (10 min at room temperature). After a blocking step with PBS-0.5 % BSA, cells were then incubated for 30 min with Alexa Fluor 546 phalloidin (5 U/ml), rinsed, and subsequently mounted under glass coverslips.

Results were analyzed by confocal microscopy (LSM510 confocal fluorescent microscope; Zeiss, Oberkochen, Germany). The primary antibodies used were rabbit anti-Cx36 (1:200, Abcam), guinea pig anti-insulin (Dako), and Alexa Fluor 546 phalloidin (Cytoskeleton). Secondary antibodies were goat anti-guinea pig Alexa Fluor 488 (1:400) and goat anti-rabbit Alexa Fluor 647 (1:400).

Statistical analysis The statistical differences of results were analyzed by a "one factor with three levels" design (SAS) or by Student's *t*-test for paired groups. *P*-values of 0.05 or less were considered significant. All results are presented as means±SE for three independent experiments from at least three parallel groups under each condition.

Results

Promotion of GSIS in MIN6 cells under 3D culture conditions

To compare the glucose responsiveness of β-cells between 3D aggregates and 2D monolayers, a 3D culture method was

designed for MIN6 cells. Under 2D conditions, the cell shape was predominantly epithelioid-like, and cells formed a monolayer throughout the culture period. Conversely, multicellular aggregate-like islet architecture was formed (Fig. 1a-d) during suspension culture in ultra-low-attachment plates for 24 h. The impact of 3D culture conditions on the GSIS of MIN6 cell-spheroids was analyzed after 4 days in culture. Cells with spheroid architecture displayed significantly improved GSIS compared with cells in monolayer culture ($P<0.0005$, Fig. 1e). Unlike the secretory insulin, the total amounts of insulin in the cell lysates were not significantly different between 2D and 3D cultures (Fig. S1a). In addition, the lysate of MIN6 aggregates was collected and analyzed by real-time reverse transcription plus PCR, which revealed that the expression of islet-related genes PDX1 and NGN3 was higher than the expression of those in the lysates of the monolayer cells ($P<0.0005$, Fig. 1f). Both the long half-life insulin mRNA (mature mRNA) and a short half-life insulin pre-mRNA species were also tested by Q-PCR (Melloul et al. 2002); however, we did not find significant differences between them under 2D and 3D conditions (Fig. S1b).

Down-regulation of RhoA activity in MIN6 cells under 3D culture conditions

The cytoskeletal arrangements of MIN6 cells cultured under 2D and 3D conditions were investigated by F-actin staining. After 4 days of culture in ultra-low-attachment 24-well plates, cells were pre-incubated in DMEM containing 5 mM glucose for 16–24 h and then in 2 mM glucose in KRBH for 1 h. Multicellular aggregates were fixed, and immunofluorescence was assessed to verify the distribution and expression of pro-insulin and F-actin. The MIN6 cells cultured under 2D conditions were used as the control. Unlike the long, well-aligned,

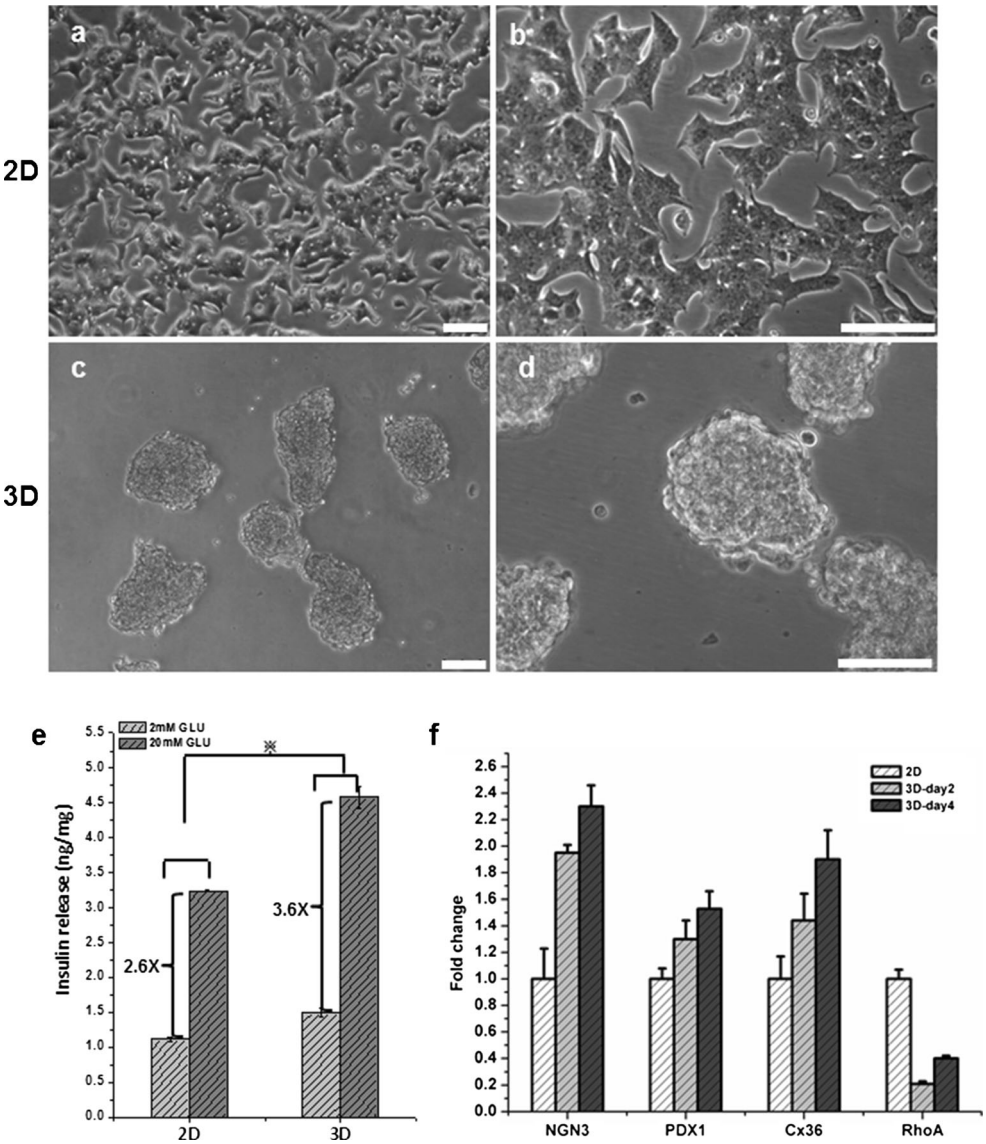

Fig. 1 Promotion of glucose-stimulated insulin secretion (GSIS) in mouse insulinoma 6 (MIN6) cells under three-dimensional (3D) culture conditions. MIN6 cells were cultured on tissue-cultured plastic (two-dimensional; *2D*) and on ultra-low-attachment (*3D*) plates, separately. **a–d** Morphological images of MIN6 cells in 2D and 3D culture (**b**, **d** higher magnification views of **a**, **c**, respectively). *Bars* 100 μm. **e** Insulin secretion from MIN6 cells in 2D and 3D culture (*GLU* glucose). Under 2D culture conditions, the MIN6 cells underwent less GSIS compared with those under 3D conditions. *Dotted X* $P<0.05$. **f** Gene expression of MIN6 cells in 2D and in 3D culture at day 2 or day 4. Quantitative polymerase chain reaction (Q-PCR) data were plotted as the fold change in expression over 2D RNA samples (equal to 1). $P<0.05$

and thickly bunched F-actin microfilament in the 2D monolayer cells, the F-actin fiber network was dramatically reorganized in 3D cultures. Confocal microscopy revealed aggregates of polymerized actin on discrete regions of the cell surface labeled by rhodamine-phalloidin (Fig. 2a-h).

Small GTPases have profound effects on actin cytoskeleton regulation. Accordingly, the contribution of RhoA activation on actin regulation in the 3D aggregates was examined. In these experiments, the proteins of 4-day aggregates and monolayer MIN6 cells were collected, and the cellular levels of active GTP-bound RhoA were determined by pull-down assay with Rhotekin-RBD beads. Our results showed that multicellular aggregates exhibited less RhoA activity than that of the monolayer MIN6 cells (Fig. 2i, j).

To examine the effect of Rho activity suppression on GSIS, RhoA-positive (CA) and negative mutant (DN) expressing vectors were stably transfected into MIN6 cells via a lentiviral transfection system, and control cells were transfected by an empty vector. The pull-down assay was used to measure RhoA activity of MIN6-CA and MIN6-DN cells. Cell immunofluorescence showed highly polymerized and well-aligned F-actin bundles in both MIN6 control and MIN6-CA cells under the 2 mM glucose basal condition, although F-actin was partially depolymerized under the stimulating culture conditions. In contrast, F-actin in the MIN6-DN cells and C3T-treated MIN6 cells were scattered in the cytoplasm, regardless of whether the culture was carried out under the 2 mM glucose basal conditions or 20 mM glucose stimulating conditions (Figs. 3c-j, S4). The insulin secretion test was performed on the lentiviral-gene-modified cells. We found that MIN6-DN cells released more insulin at high-glucose concentrations ($P<0.01$, Fig. 3k). To distinguish the effects of gene modification and to confirm the impact of RhoA activity on MIN6 cell function, monolayer MIN6 cells were treated by RhoA inhibitor C3 in a GSIS test. Results showed that insulin secretion was also significantly increased under both low- and high-glucose concentrations together with RhoA activity inhibition (Fig. 3l).

ROCK is a downstream effector of GTP-bound RhoA. To further investigate the role of Rho/ROCK on MIN6 cell function, MIN6 cells were continuously treated with ROCK inhibitor Y27632 for 4 days. Unexpectedly, MIN6 cells in both 2D and 3D cultures secreted insulin upon high glucose stimulation, but the total insulin produced decreased (Fig. S2). We

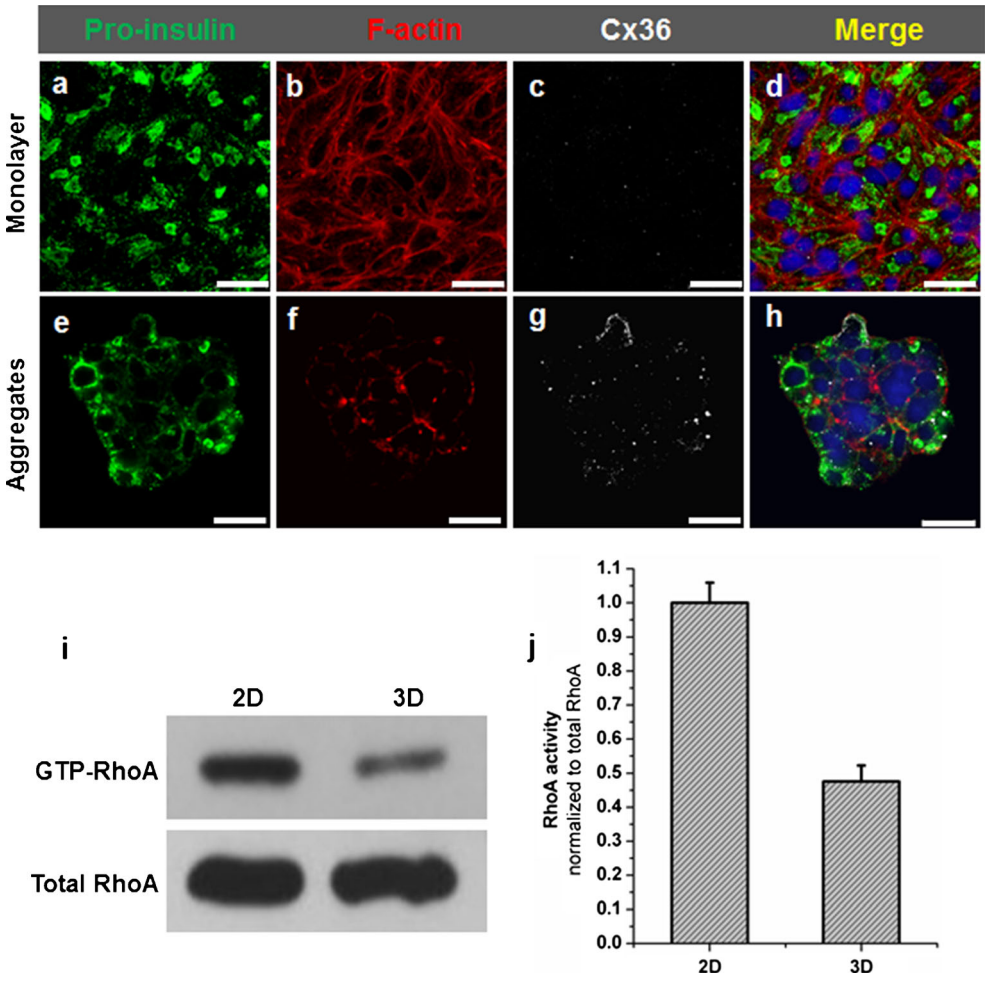

Fig. 2 Cytoskeleton reconstruction in 3D cells. During cytoskeleton reconstruction in 3D cells, RhoA activity is simultaneously down-regulated. **a–h** Immunofluorescent staining of F-actin, pro-insulin, and connexin 36 (*Cx36*) in cells grown in 2D and 3D culture (*green* pro-insulin, *red* F-actin, *white* Cx36, *blue* nuclei). *Bars* 20 μm. **i**, **j** RhoA activation (GTP-bound RhoA/total RhoA) in cells grown in 2D and 3D culture. **i** Representative pulldown. **j** Quantification

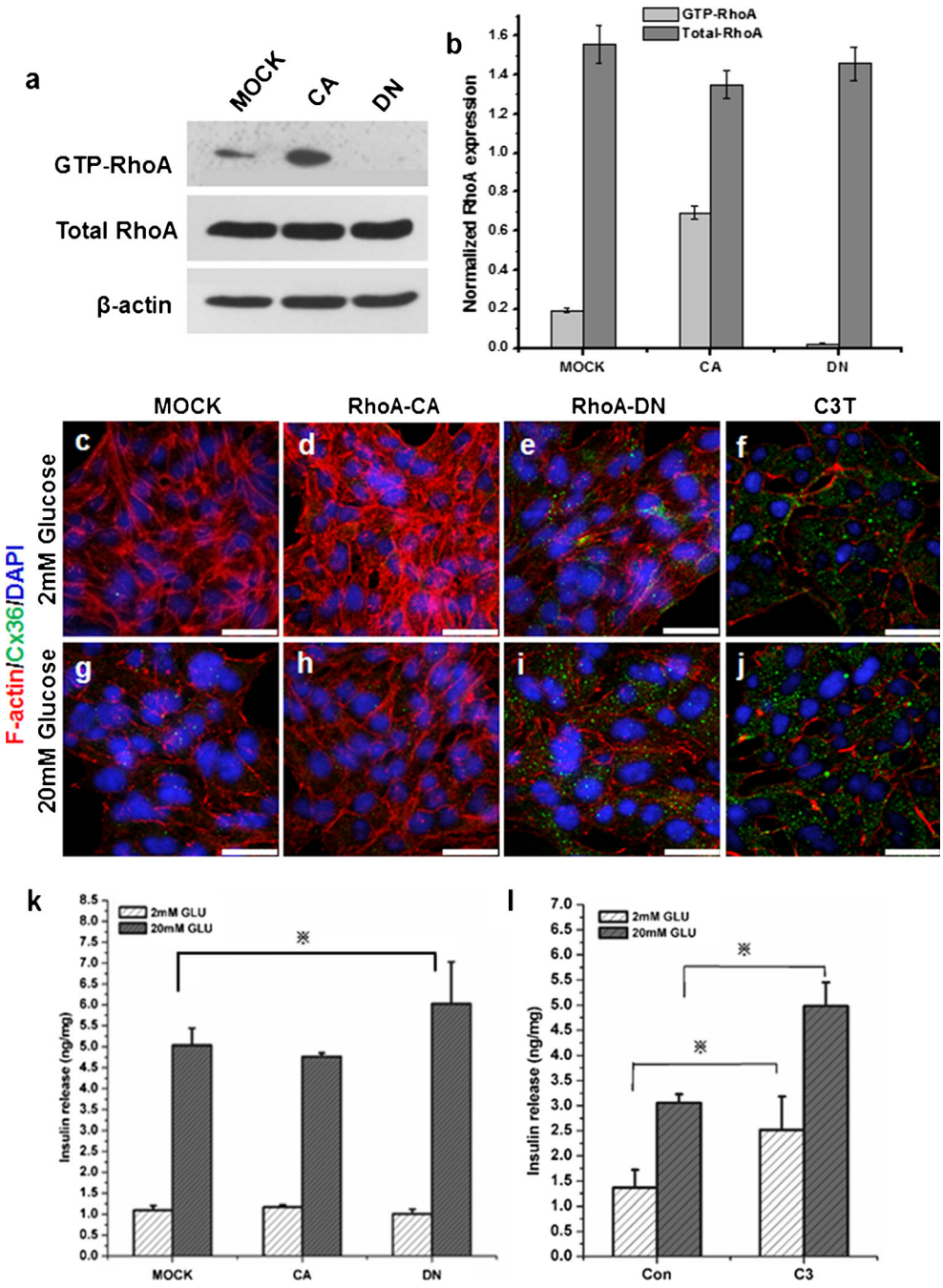

Fig. 3 Down-regulation of RhoA activity promotes GSIS, and expression of Cx36 is accordingly up-regulated. **a**, **b** RhoA activation (GTP-bound RhoA/total RhoA) in MIN6 cells transfected with RhoA-CA-expressing (*CA*) and RhoA-DN-expressing (*DN*) vectors (*MOCK* mock-transfected MIN6 cells as a control). **a** Representative pulldown. **b** Quantification ($n=3$, *error bars* ±SE). **c–j** Immunofluorescent staining of F-actin and Cx36 in gene-modified MIN6 cells and C3T-treated cells under 2 mM glucose basal conditions or 20 mM glucose stimulating conditions (*green* Cx36, *red* F-actin, *blue* nuclei, *MOCK* mock-transfected MIN6 cells as a control, *RhoA-CA* MIN6 cells transfected with constitutively active RhoA mutant-expressing vectors, *RhoA-DN* MIN6 cells transfected with dominant negative RhoA mutant-expressing vectors, *C3T* MIN6 cells treated with Rho inhibitor C3 transferase). *Bars* 20 μm. **k** Insulin secretion from gene modified MIN6 cells (*GLU* glucose). *Dotted X* $P<0.01$. **l** Insulin secretion from MIN6 cells treated by RhoA inhibitor C3T. *Dotted X* $P<0.01$

then used Y27632 only for the insulin secretion test to verify whether the inhibition of ROCK improved glucose-stimulated insulin secretion acutely. The results showed that Y27632 did not increase the insulin released from MIN6 cells at the lower (2 mM) concentration of glucose; however, it did induce more insulin release with increasing Y27632 doses in MIN6 cells at the higher (20 mM) concentration of glucose (Fig. 4a). In terms of the total amounts of insulin in the cell lysates, no significant difference was observed (Fig. S3a). Furthermore, the effect was almost equivalent when MIN6 cells were treated by 50 μM Y27632 or cultured under 3D conditions. Immunofluorescence observation also confirmed the effect of Y27632, as F-actin was depolymerized in MIN6 cells treated with Y27632 for 2 h (Figs. 4b-e, S5). The status of the depolymerized condition was maintained until the withdrawal of Y27632 (data not shown). The influence of Y27632 on gene expression was then tested. Endocrine-related genes such as PDX1 and NGN3 were up-regulated when Y27632 was continuously added in prolonged cultures (Fig. 5a) or with increasing doses (Fig. 5b), but neither mature mRNA nor pre-mRNA species showed significant changes (Fig. S3b). The effects of Y27632 on PDX1 and NGN3

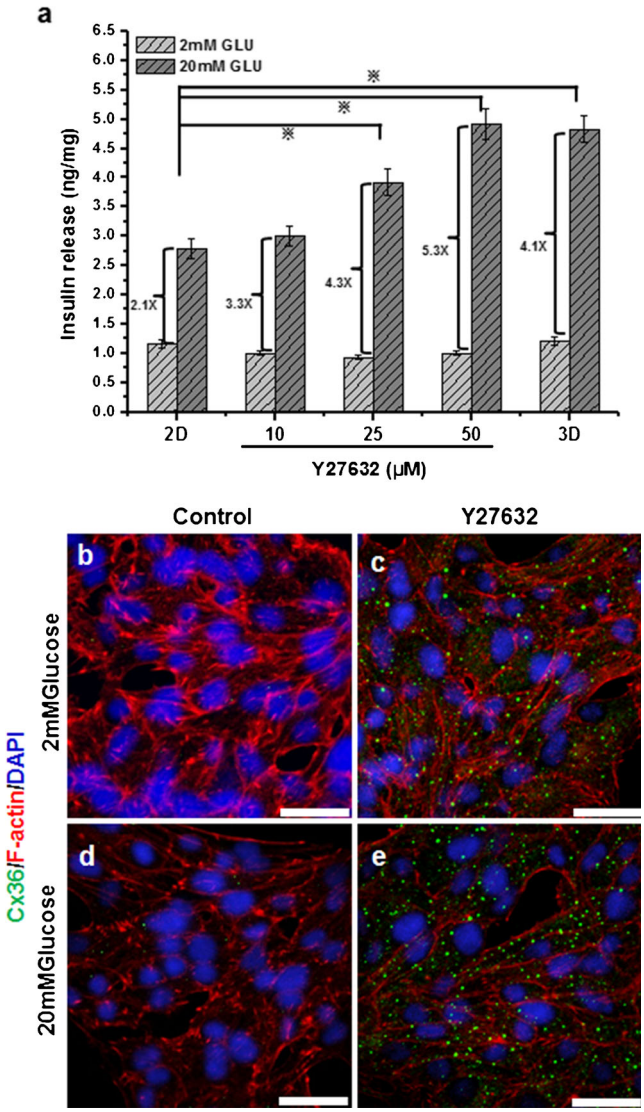

Fig. 4 Rho-ROCK pathway is involved in cytoskeleton reconstruction, and Cx36 is up-regulated during the reconstruction. **a** Insulin secretion from MIN6 cells treated by ROCK inhibitor Y27632. The GSIS of MIN6 cells treated with various dosages of Y27632 and under 3D conditions was higher than that under 2D conditions (*GLU* glucose). *Dotted X P*<0.05. **b–e** Immunofluorescent staining of F-actin and Cx36 in MIN6 cells treated by Y27632 under 2 mM glucose basal conditions or 20 mM glucose stimulating conditions (*green* Cx36, *red* F-actin, *blue* nucleus). *Bars* 20 μm

expression were also equivalent to those under 3D culture conditions (Figs. 1e, 5a, b).

Requirement of Cx36 for effects of Rho-ROCK pathway on insulin secretion

The expression of Cx36 in MIN6 cells was examined in both monolayer cells and 3D aggregates. Immunofluorescent staining and Q-PCR data showed that Cx36 expression was up-regulated under 3D culture conditions (Figs. 1f, 2a-h). Western blot analysis was conducted with cell extracts of the two conditions after 4, 24, and 48 h of culture. Compared with that in the monolayer cultured cells, the expression of Cx36 in the 3D MIN6 cells cultured for 48 h was significantly increased (Fig. 5c, d). Cx36 was also increased when RhoA or ROCK was inactivated. Careful examination of the distribution of Cx36 in immunofluorescently stained MIN6 cells that were gene-modified (Fig. 3c-j) or Y27632-treated (Fig. 4b-e) revealed that more connections were formed during re-aggregation. In addition, Q-PCR and Western blot analyses showed that the levels of Cx36 in the ROCK-inhibitor-treated MIN6 cells were significantly increased (Fig. 5a, b, e, f). To determine whether increasing Cx36 expression was required for insulin secretion, three siRNAs were designed to knock down Cx36 expression within MIN6 cells. The Cx36 proteins were analyzed by Western blots after 3 days of transfection with Cx36-siRNA1-expressing MIN6 cells found to be lower compared to the control siRNA-expressing cells (Fig. 6a, b). Thus Cx36 siRNA1 was used in the insulin secretion test. Results showed that Cx36 siRNA1 not only decreased higher glucose stimulated insulin secretion, but also affected Y27632- and C3-treated MIN6 cells in which ROCK and RhoA activities were down-regulated accordingly (Fig. 6c).

Discussion

The integrated secretory response of intact islets of Langerhans cells is greater than that of dispersed islet cells, and re-aggregation improves secretory responsiveness, thereby suggesting that intra-islet interactions are essential for normal secretory responses (Hauge-Evans et al. 1999). In addition, euglycemia depends on a constituent ratio of various cell populations inside pancreatic islets and the cross-talk amongst them. Thus, the maintenance of normal islet structure is the basis of glucoregulatory functions. For research purposes, the MIN6 insulinoma cell line routinely undergoes 2D culture as an adherent monolayer on tissue culture plastic, with cells connecting to neighboring cells, but with the absence of essential cellular functions that are present in tissues (in vivo) because the cells have to adjust to artificially flat and rigid surfaces. In contrast, 3D culturing has many advantages, with cells connecting to the cell matrix/neighboring cells in a 3D space that mimics the in vivo microenvironment. The lineage restriction of embryonic stem cells to specific mature cells has also been shown to be more efficiently achieved under 3D culture conditions (Liu et al. 2006; Pelto et al. 2013). To improve studies of the effects of structure on gene expression and functional responses within islets, we have used 3D culture-formed spherical islet-like aggregates of MIN6 cells. Cellular spheroids are simple 3D systems that take advantage of the natural tendency of many cell types to aggregate (Pampaloni et al. 2007). The ability of dispersed islet cell or clonal β-cell lines to aggregate or re-aggregate

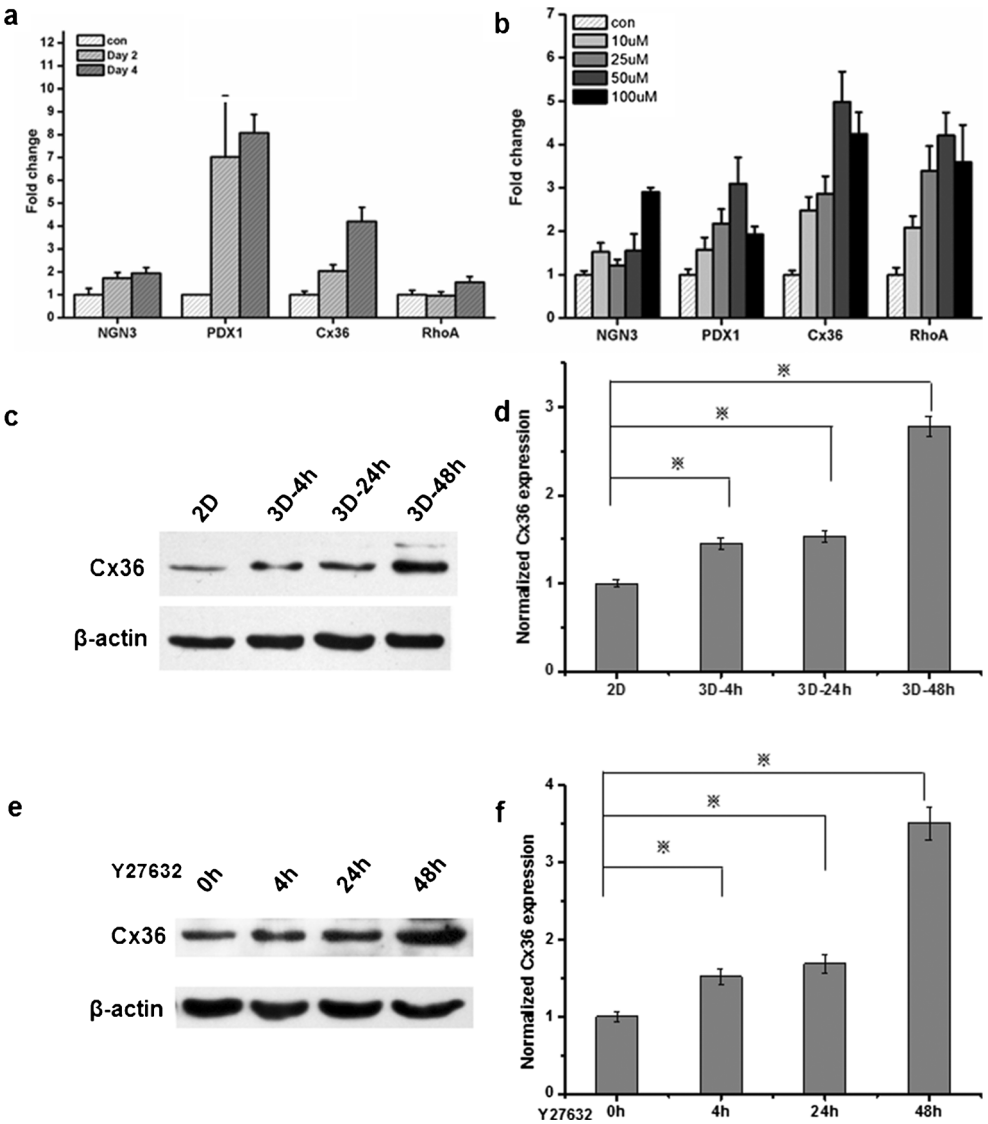

Fig. 5 Expression of Cx36 is increased under 3D conditions or upon ROCK inhibition. **a**, **b** Gene expression in Y27632-treated MIN6 cells. Islet-related genes are up-regulated in Y27632-treated cells at increasing doses or under prolonged culture. Q-PCR data were plotted as fold changes in expression over control RNA samples (equal to 1). **a** Gene up-regulation in MIN6 cells after treatment with Y27632 for 2 and 4 days ($P<0.05$). **b** Gene up-regulation of MIN6 after treatment with increasing doses of Y27632 for 4 days ($P<0.05$). **c**–**f** Western blot analysis of Cx36 expression in MIN6 cells cultured under 3D conditions or treated with Y-27632. **c**, **d** Cx36 expression in MIN6 cells cultured under 3D conditions or 2D conditions for 4, 24, and 48 h. **c** Representative Western blot. **d** Quantification. *Dotted X* $P<0.05$ ($n=3$, *error bars* ±SE). **e**, **f** Cx36 expression in MIN6 cells treated with Y-27632 for 0, 4, 24, and 48 h. **e** Representative Western blot. **f** Quantification. *Dotted X* $P<0.05$

in vitro has been reported previously (Halban et al. 1987; Hauge-Evans et al. 1999). MIN6 cells cultured in the current 3D system easily form aggregates, and the MIN6 cells grown as aggregates release more insulin than those in 2D cultures. In addition, endocrine-related genes, such as PDX1 and NGN3, are up-regulated under the 3D culture conditions. In vitro 3D culture restores the cell-cell interactions and the cell-cell communications that occur in vivo, all of which are important for GSIS and the gene expression of the islet cells. Prior studies have established that the distinct functional responses between monolayer islet cells and islet aggregates are caused by the different free Ca^{2+} concentrations in cells (Hauge-Evans et al. 1999). However, correlations between cytoskeletal state and gap junction functions of β-cells with their secretion have remained obscure.

When MIN6 cells form cell aggregates, the morphology of the cells has a profound effect on their cytoskeleton, and the disruption and reorganization of filamentous actin (F-actin) is required. Ultrastructural analysis has indicated that F-actin is organized as a dense web beneath the plasma membrane. Numerous studies with F-actin disrupting agents such as clostridial toxins and cytochalasins have shown enhanced secretagogue-induced insulin secretion, suggesting that F-actin blocks granule movement (Wang and Thurmond 2009). To examine the remodeling of F-actin when cell morphology is changed in 3D aggregates, we have analyzed the distribution of insulin and F-actin in 2D- and 3D-cultured cells by confocal immunofluorescence. Unlike the long, well-aligned, and thickly bunched F-actin fibers in the 2D monolayer cells, the F-actin fiber network is dramatically re-organized as aggregates of polymerized actin in discrete regions of the cell surface, as indicated by labeling with rhodamine-phalloidin.

Actin remodeling in several cell types is regulated by the small Rho-family of GTPases. This family of proteins is a subfamily of the Ras-related GTPase superfamily and contains more than ten members in mammals, including Rho,

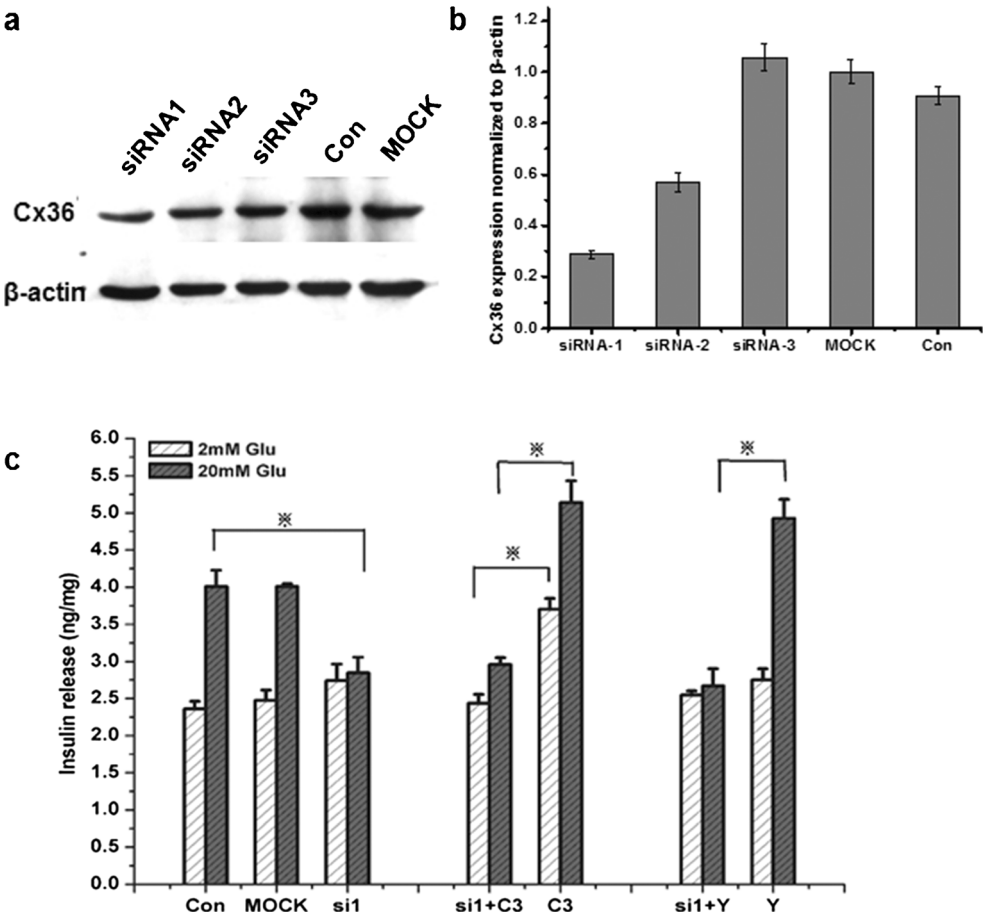

Fig. 6 Requirement of Cx36 for the effects of Rho-ROCK pathway on insulin secretion. **a**, **b** Western blot analysis of Cx36 in MIN6 cells transfected with control siRNA (*Con*) or Cx36 siRNA 1 (*siRNA1* in **a**, *siRNA-1* in **b**), Cx36 siRNA 2 (*siRNA2* in **a**, *siRNA-2* in **b**), or Cx36 siRNA 3 (*siRNA3* in **a**, *siRNA-3* in **b**). **a** Representative Western blot. **b** Quantification. **c** Insulin secretion from MIN6 cells transfected with control siRNA (*Con*) or Cx36 siRNA 1 (*si1*), from mock-transfected MIN6 cells (*MOCK*), and from control cells treated with Y27632 (*Y*) or C3. *Dotted X P*<0.05

Rac, and Cdc42. In the 1990s, Cdc42 and Rac1, in particular, were found to participate in insulin secretion and were co-localized in the insulin-containing granule. However, relatively little was known regarding the effects of Rho on insulin secretion (Wang and Thurmond 2009). The regulators of F-actin, namely small GTPase RhoA and its effector ROCK, have now been taken into consideration, since studies have shown that insulin secretion is related to the inactivation of RhoA/ROCK when F-actin organization is disrupted at the same time. Based on our previous findings that RhoA/ROCK regulates both cell morphology mobility and stem cell fate decision (Yao et al. 2009), we conclude that the activity of RhoA/ROCK is down-regulated in MIN6 cell spheroids under 3D culture conditions. Further, the increase of insulin secretion is also RhoA/ROCK activity related, although a high glucose concentration is absolutely necessary. In particular, when we treat MIN6 cells with the ROCK inhibitor Y27632 for 4 days, we have not found the anticipated insulin-increasing result. This phenomenon is similar to that reported in the study of Racchetti et al. (2012) who have found that Y27632 can promote enlargeosome secretion from astrocytes, and that the repeated stimulation of Y27632 might exhaust the enlargeosome granules, which then decrease their secretion activity . We infer that long-term stimulation of Y27632 can also exhaust insulin secretion in MIN6 cells. We assume that that is the reason that insulin secretion decreases with the increasing dosage of Y27632 in the stimulated insulin-releasing tests after 4 days of Y27632 administration.

In most tissues, gap junctions are important in the control of cell proliferation, differentiation, and regeneration. Gap junction channels connecting the cytoplasm of adjoining cells are formed by the interaction of the transmembrane proteins, the Cxs, which form a “connexon” on one cell, with the Cxs of a connexon on an adjoining cell. The turnover time of Cxs is reported to be short, with a half-life of only 1.3–2 h, and the inhibition of ROCK results in an increase in the number of Cx43 gap junctions and in cell-cell communication (Anderson et al. 2002). The β-cells within an islet are connected via gap junctions composed of the Cx36 protein and are electrically coupled. This raises the possibility that cell-cell contact among β-cells in an islet promotes gap junction communication, thereby coordinating the heterogeneous responses of individual cells and, in turn, producing the observed integrated secretory response of the whole islet.

Since 3D culture conditions can enhance cell-cell and cell-matrix interactions, more cell connections have been found in the cell aggregates in our study. Moreover, up-regulated Cx36 gene expression and more gap junction formation by Cx36

have been detected in the 3D cultured MIN6 cells. Previous research has suggested that Cx36 loss can lead to pancreatic dysfunction (Speier et al. 2007). Both sets of data suggest an important role of the gap junction protein Cx36 in insulin secretion. In our study, we have also found that, after Cx36 knockdown, the secretion of insulin is reduced, regardless of whether RhoA/ROCK is inactivated. This finding suggests that Cx36 is involved in the RhoA/ROCK-regulated insulin secretion pathway. However, further research is required to clarify this relationship.

In summary, we have established a 3D culture system in which cells form islet-like aggregates, show high expression of PDX1 and NGN3 genes, and secrete more insulin. Moreover, the RhoA/ROCK pathway and Cx36 protein have been demonstrated to be involved in aggregate formation and insulin secretion under 3D culture conditions. Our findings provide a possible basis for the induced differentiation of stem cells into functional insulin-secretion pancreatic β-cells.

References

Ahren B, Filipsson K (2000) The effects of PACAP on insulin secretion and glucose disposal are altered by adrenalectomy in mice. Ann N Y Acad Sci 921:251–258

Anderson SC, Stone C, Tkach L, SundarRaj N (2002) Rho and Rho-kinase (ROCK) signaling in adherens and gap junction assembly in corneal epithelium. Invest Ophthalmol Vis Sci 43:978–986

Bell GI, Polonsky KS (2001) Diabetes mellitus and genetically programmed defects in beta-cell function. Nature 414:788–791

Benninger RK, Head WS, Zhang M, Satin LS, Piston DW (2011) Gap junctions and other mechanisms of cell-cell communication regulate basal insulin secretion in the pancreatic islet. J Physiol (Lond) 589: 5453–5466

Bhandari DR, Seo KW, Sun B, Seo MS, Kim HS, Seo YJ, Marcin J, Forraz N, Roy HL, Larry D, Colin M, Kang KS (2011) The simplest method for in vitro beta-cell production from human adult stem cells. Differentiation 82:144–152

Bosco D, Haefliger JA, Meda P (2011) Connexins: key mediators of endocrine function. Physiol Rev 91:1393–1445

Carvalho CP, Oliveira RB, Britan A, Santos-Silva JC, Boschero AC, Meda P, Collares-Buzato CB (2012) Impaired beta-cell-beta-cell coupling mediated by Cx36 gap junctions in prediabetic mice. Am J Physiol Endocrinol Metab 303:E144–E151

Furukawa N, Ongusaha P, Jahng WJ, Araki K, Choi CS, Kim HJ, Lee YH, Kaibuchi K, Kahn BB, Masuzaki H, Kim JK, Lee SW, Kim YB (2005) Role of Rho-kinase in regulation of insulin action and glucose homeostasis. Cell Metab 2:119–129

Grapin-Botton A, Melton DA (2000) Endoderm development: from patterning to organogenesis. Trends Genet 16:124–130

Guo-Parke H, McCluskey JT, Kelly C, Hamid M, McClenaghan NH, Flatt PR (2012) Configuration of electrofusion-derived human insulin-secreting cell line as pseudoislets enhances functionality and therapeutic utility. J Endocrinol 214:257–265

Halban PA, Powers SL, George KL, Bonner-Weir S (1987) Spontaneous reassociation of dispersed adult rat pancreatic islet cells into aggregates with three-dimensional architecture typical of native islets. Diabetes 36:783–790

Hammar E, Tomas A, Bosco D, Halban PA (2009) Role of the Rho-ROCK (Rho-associated kinase) signaling pathway in the regulation of pancreatic beta-cell function. Endocrinology 150:2072–2079

Hauge-Evans AC, Squires PE, Persaud SJ, Jones PM (1999) Pancreatic beta-cell-to-beta-cell interactions are required for integrated responses to nutrient stimuli: enhanced Ca^{2+} and insulin secretory responses of MIN6 pseudoislets. Diabetes 48:1402–1408

Head WS, Orseth ML, Nunemaker CS, Satin LS, Piston DW, Benninger RK (2012) Connexin-36 gap junctions regulate in vivo first- and second-phase insulin secretion dynamics and glucose tolerance in the conscious mouse. Diabetes 61:1700–1707

Henquin JC (2000) Triggering and amplifying pathways of regulation of insulin secretion by glucose. Diabetes 49:1751–1760

Kowluru A (2010) Small G proteins in islet beta-cell function. Endocr Rev 31:52–78

Li J, Luo R, Kowluru A, Li G (2004) Novel regulation by Rac1 of glucose- and forskolin-induced insulin secretion in INS-1 beta-cells. Am J Physiol Endocrinol Metab 286:E818–E827

Liu H, Lin J, Roy K (2006) Effect of 3D scaffold and dynamic culture condition on the global gene expression profile of mouse embryonic stem cells. Biomaterials 27:5978–5989

Luther MJ, Hauge-Evans A, Souza KL, Jorns A, Lenzen S, Persaud SJ, Jones PM (2006) MIN6 beta-cell-beta-cell interactions influence insulin secretory responses to nutrients and non-nutrients. Biochem Biophys Res Commun 343:99–104

Meda P (1996) Role of intercellular communication via gap junctions in insulin secretion. Ann Endocrinol (Paris) 57:481–483

Meda P, Bosco D, Chanson M, Giordano E, Vallar L, Wollheim C, Orci L (1990) Rapid and reversible secretion changes during uncoupling of rat insulin-producing cells. J Clin Invest 86:759–768

Melloul D, Marshak S, Cerasi E (2002) Regulation of insulin gene transcription. Diabetologia 45:309–326

Michon L, Nlend NR, Bavamian S, Bischoff L, Boucard N, Caille D, Cancela J, Charollais A, Charpantier E, Klee P, Peyrou M, Populaire C, Zulianello L, Meda P (2005) Involvement of gap junctional communication in secretion. Biochim Biophys Acta 1719:82–101

Nakamura Y, Kaneto H, Miyatsuka T, Matsuoka TA, Matsuhisa M, Node K, Hori M, Yamasaki Y (2006) Marked increase of insulin gene transcription by suppression of the Rho/Rho-kinase pathway. Biochem Biophys Res Commun 350:68–73

Nevins AK, Thurmond DC (2003) Glucose regulates the cortical actin network through modulation of Cdc42 cycling to stimulate insulin secretion. Am J Physiol Cell Physiol 285:C698–C710

Nevins AK, Thurmond DC (2005) A direct interaction between Cdc42 and vesicle-associated membrane protein 2 regulates SNARE-dependent insulin exocytosis. J Biol Chem 280:1944–1952

Pampaloni F, Reynaud EG, Stelzer EH (2007) The third dimension bridges the gap between cell culture and live tissue. Nat Rev Mol Cell Biol 8:839–845

Pelto J, Bjorninen M, Palli A, Talvitie E, Hyttinen JA, Mannerstrom B, Suuronen SR, Kellomaki M, Miettinen S, Haimi S (2013) Novel polypyrrole coated polylactide scaffolds enhance adipose stem cell proliferation and early osteogenic differentiation. Tissue Eng Part A 19:882–892

Racchetti G, D'Alessandro R, Meldolesi J (2012) Astrocyte stellation, a process dependent on Rac1 is sustained by the regulated exocytosis of enlargeosomes. Glia 60:465–475

Ravier MA, Guldenagel M, Charollais A, Gjinovci A, Caille D, Sohl G, Wollheim CB, Willecke K, Henquin JC, Meda P (2005) Loss of connexin36 channels alters beta-cell coupling, islet synchronization of glucose-induced Ca^{2+} and insulin oscillations, and basal insulin release. Diabetes 54:1798–1807

Ridley AJ (2006) Rho GTPases and actin dynamics in membrane protrusions and vesicle trafficking. Trends Cell Biol 16:522–529

Scemes E, Spray DC, Meda P (2009) Connexins, pannexins, innexins: novel roles of "hemi-channels". Pflugers Arch 457:1207–1226

Song P, Zhang M, Wang S, Xu J, Choi HC, Zou MH (2009) Thromboxane A2 receptor activates a Rho-associated kinase/LKB1/PTEN pathway to attenuate endothelium insulin signaling. J Biol Chem 284:17120–17128

Speier S, Gjinovci A, Charollais A, Meda P, Rupnik M (2007) Cx36-mediated coupling reduces beta-cell heterogeneity, confines the stimulating glucose concentration range, and affects insulin release kinetics. Diabetes 56:1078–1086

Thurmond DC, Gonelle-Gispert C, Furukawa M, Halban PA, Pessin JE (2003) Glucose-stimulated insulin secretion is coupled to the interaction of actin with the t-SNARE (target membrane soluble N-ethylmaleimide-sensitive factor attachment protein receptor protein) complex. Mol Endocrinol 17:732–742

Villa-Diaz LG, Ross AM, Lahann J, Krebsbach PH (2013) Concise review: the evolution of human pluripotent stem cell culture: from feeder cells to synthetic coatings. Stem Cells 31:1-7

Wang X, Ye K (2009) Three-dimensional differentiation of embryonic stem cells into islet-like insulin-producing clusters. Tissue Eng Part A 15:1941–1952

Wang Z, Thurmond DC (2009) Mechanisms of biphasic insulin-granule exocytosis—roles of the cytoskeleton, small GTPases and SNARE proteins. J Cell Sci 122:893–903

Yao H, Jia Y, Zhou J, Wang J, Li Y, Wang Y, Yue W, Pei X (2009) RhoA promotes differentiation of WB-F344 cells into the biliary lineage. Differentiation 77:154–161